

CHAPTER 4.....

RESULTS AND DISCUSSION

Applications of Transition Metal-Polyaniline
Nanocomposites as Sensors

4.1 Introduction :

A chemical sensor can be defined as a device, which responds to a particular analyte in a selective way through a chemical reaction and can be used for qualitative or quantitative determination of an analyte. Chemical sensing is a critical aspect of life. Our ability to sense the environment is based on different sense organs present in our body such as the eyes, nose, skin, ears and tongue. Apart from the above sense organs, man requires other types of sensors in view of the increasing concern about pollution around us, human health and safety aspects. The rapid advancement in science and instrumentation has shown that manufactured chemicals and by-products have been introduced into almost every aspect of our environment and lives. Therefore, the quest for determining concentration of pollutants up to a minimum permissible limit with simple technology at lower costs has become very important. To fulfil all the requirements, a chemical sensor is a good option e.g. the sensors used to determine the percentage of CO and NO_x from the exhaust of the automobiles are very simple to handle and compact to carry. The sensing technology has its base in the chemistry and is an interdisciplinary branch of science covering areas like inorganic chemistry, organic chemistry, materials science, physics and molecular biology.

4.1.1 Principle of solid state sensor :

Present day gas sensing technology is mainly based on solid state devices which combine simple construction with low cost and high sensitivity [75]. The chemical sensor is built from two basic components viz; a sensing element where selective physico-chemical changes take place upon interacting with analyte, and the transducer which detects the change and converts the signal into an electrical output of measurable quantity that can be amplified, processed and displayed in a suitable form. Interaction of analyte with the sensing element produces a signal in the form of a change in the physico-chemical property of the sensing element such as change in colour of fluorescent light, a change in electric potential at the surface, flow of electrons, the production of heat or change in the oscillator frequency of the crystal. The transducer reports this signal and translates the magnitude of signal into a measure of amount of analyte. The large number of possibilities also lead to a number of different types of devices as given in Table 4.1. Multi faceted solid state sensor technologies have been developed based on the similar principle of sensing.. The successful performance of a chemical sensor depends on the appropriate choice of sensing elements and transducer. Important thing to be considered is that the interaction of the analyte with sensor should be reversible and reproducible.

Table 4.1 Type of Sensors and Respective Physical Changes Occurring During Sensing.

Type of device	Physical change
Pt wire Thermopiles Thin film resistors Micro calorimeters	Heat generation
Semiconducting oxides Conducting polymers Nanocomposites	Conductivity
Fibre optics : reflection , interferometry Adsorption : fluorescence. Thin films : reflection	Optical
Field effect devices : diodes, capacitors, transistors, Kelvin probes	Work function electrical polarisation
Capacitors	Dielectric permittivity
Quartz crystal micro balance Surface acoustic waves	Mass

Presently, efforts are on, towards synthesizing new materials like organic conducting polymers and their composites, blends etc. to obtain the required properties at minimum expenses. These polymers exhibit novel conducting and redox properties due to the presence of π conjugated system in their structure. Several reports are available proposing the use of conducting polymers like polyaniline, polypyrrole and polythiophene as sensors for chemical vapours [76-78]. Kanatzidis [79] has reviewed the use of polyaniline and polypyrrole as sensor for various volatile organic vapours. However, the sensitivity and processibility of these pristine polymers was found to be poor resulting in difficulty in their application as sensor. Therefore, latter trials involved the use of various organic and inorganic substances as dopants for these polymers to achieve better selectivity, conductivity and processibility. For example, camphor sulphonic acid (CSA), dodecyl benzene sulphonic acid DBSA and long chain organic acids as dopants, render better processibility and increased sensitivity towards many vapours compared to pristine polymers [80-81]. Also, enzyme-immobilized polyaniline or polypyrrole are being used as bio-chemical sensors for determining the concentration of various metabolites in the sample e.g. enzyme immobilized on polyaniline is used for determining the concentration of glucose in given solution [82]. Further developments in this field are the

synthesis of nanocomposites comprising transition metals and conducting polymers [83-84]. The nanocomposites due to their unique activities are expected to play a key role by providing new dimensions in sensing, thereby enabling a wider range of species to be determined in a much more complex environment.

4.1.2 Pd, Au and Ag-Polyaniline nanocomposites as organic

vapour sensors:

Chemical sensors find applications in many industries like automotive, chemical, refineries etc. At the same time, they are equally applicable in the medical field to determine the pH, sugar, concentrations of sodium or potassium and oxygen in blood [93-95]. They have been useful for monitoring the pollution levels of pollutants in air and water [96]. A considerable sensitivity and selectivity is offered by enzyme immobilized chemical biosensors and are under developmental stage for their applications [97].

Presently, Pd-Polyaniline Au-Polyaniline and Ag-Polyaniline nanocomposites have been utilized as organic vapour sensors. These nanocomposites were tested for many vapours e.g. ammonia, different alcohols, chloroform, carbon tetrachloride and different percentages of relative humidities. The selectivity of these nanocomposites towards particular analyte could be decided on the basis of their response while,

the sensitivity of the nanocomposite was tested by sensing various concentrations of the analyte vapours.

The sensing activity of a sensor is expected to be a purely surface related phenomenon. Surface characteristics and chemical nature play an important role during adsorption and desorption of the analyte molecule on the surface of the sensor. In case of metal-polymer nanocomposites, a chemical reaction occurs involving proton exchange or hydrogen bonding between the surface of the sensor and the analyte molecule. These interactions lead to a modification in the structure of polyaniline, which could be easily detected with the help of FT-IR spectroscopy. Based on these modifications in the FT-IR spectra, the sensing mechanism of the sensor towards the analyte could be predicted.

4.2 Pd-Polyaniline Nanocomposite as a Methanol Vapour Sensor :

The preliminary results of the sensing tests of the Pd-pani nanocomposite revealed its sensitivity towards methanol vapours. Therefore, further experiments were carried out only for methanol. Figure 4.1 depicts the response curves ($\Delta R/R_0$) obtained with the blank polyaniline (Pani) exposed to saturated methanol vapours (2000 ppm) and the Pd-Pani nanocomposite subjected to different concentrations of methanol vapours. As observed from Fig. 4.1, although the response of blank Pani (curve A) is reproducible, the magnitude is relatively low $\sim 10^1$

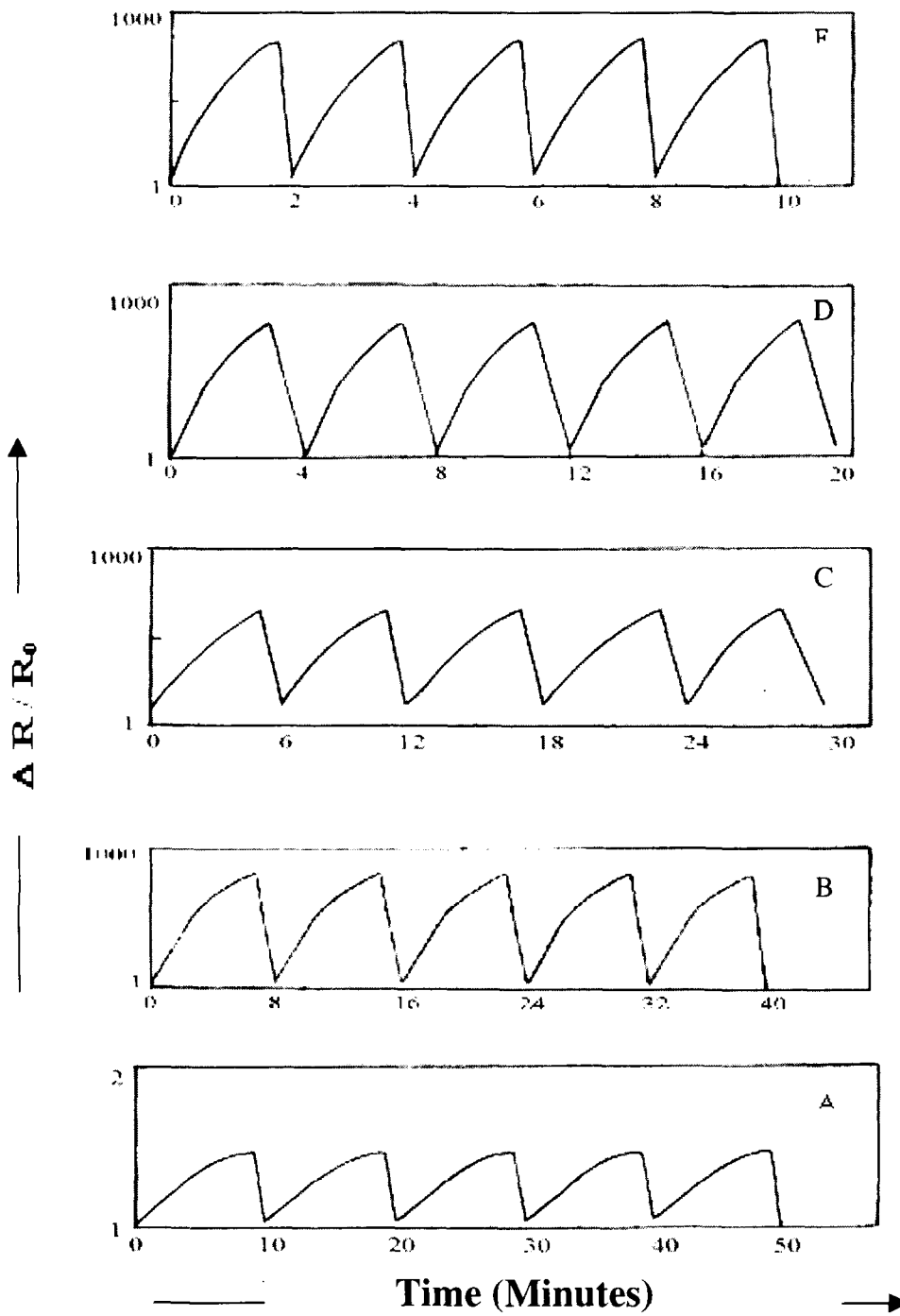


Fig. 4.1 Pd-Pani nanocomposite exposed to various concentrations of methanol such as A) 50 ppm, B) 100 ppm and C) 2000 ppm.

and the response time is also seen to extend up to several minutes. Whereas, in the case of Pd-Pani nanocomposite one can observe a rapid response in the presence of methanol as well as in air, i.e. for the forward and backward cycle (Fig. 4.1, curves B-F). In addition to this, the magnitude of the response is found to be of the order of $\sim 10^3$ (Fig. 4.2) with the resistance changing from $\sim 14 \text{ K}\Omega$ to $40 \text{ M}\Omega$. However, the nanocomposite is seen to exhibit a linear response up to 10 ppm beyond which the change in resistance is found to be identical independent of the concentration. Further, the sensitivity of the nanocomposite was determined by a graphical method. The sensitivity was found to be $\sim 8.9 \times 10^5 \text{ }\Omega \text{ ppm}^{-1}$, as calculated from the slope of a plot of resistance versus concentration. The linear increase in sensitivity was observed up to 10 ppm methanol and thereafter saturation was observed. Moreover, the response time is observed to decrease from 8 to 2 min. as the concentration of methanol increases from 1 ppm to 2000 ppm.

These results reveal that the Pd-Pani nanocomposite serves as an efficient sensor compared to blank Pani, which can be accounted in terms of the enhanced degree of interactions between the nanocomposite and the vapours due to the larger surface area provided by the Pd nanoparticles present in the nanocomposite near the imine nitrogens [98]. The reproducibility in the response at each concentration in case of the

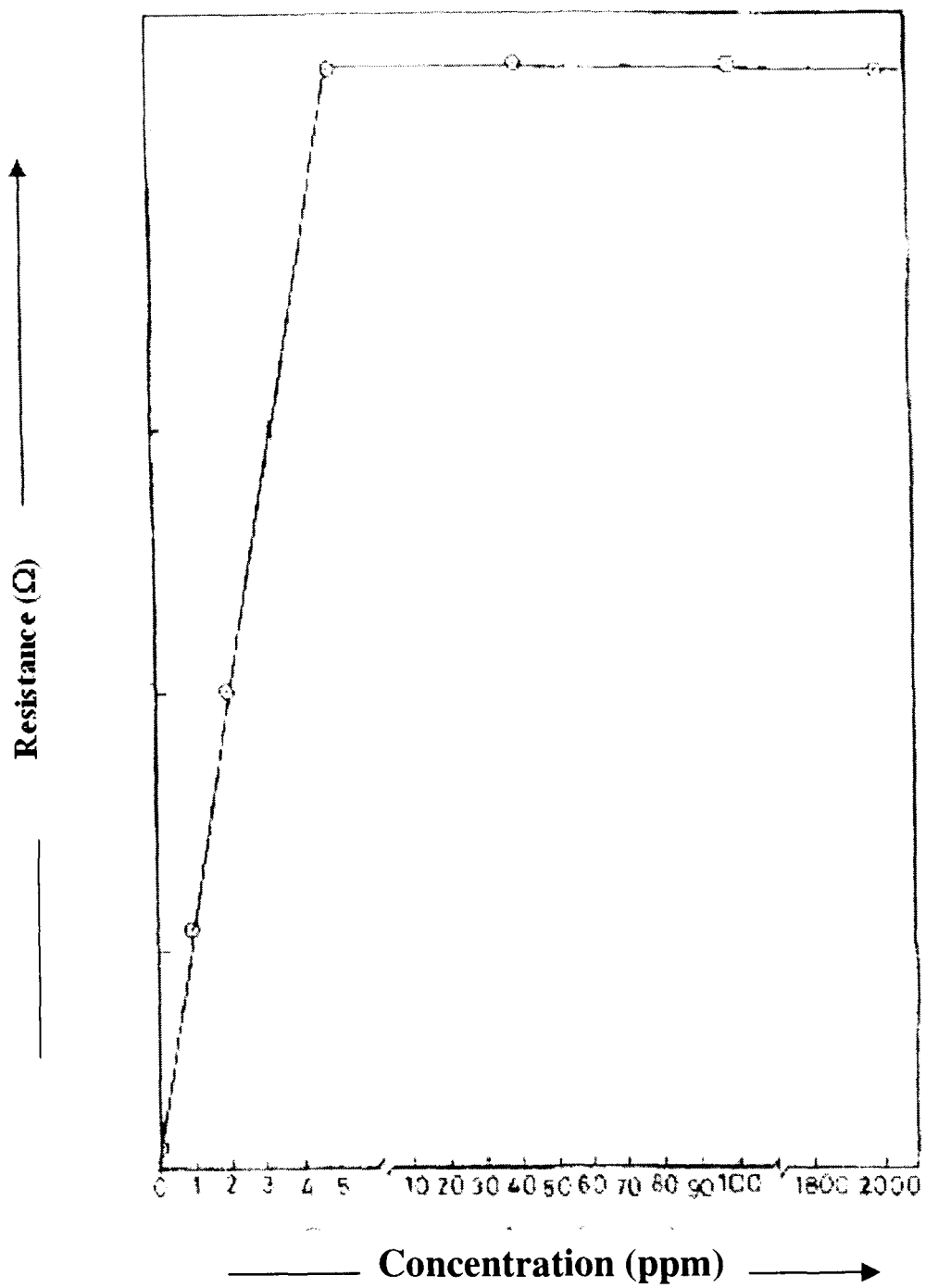


Fig. 4.2 A plot of resistance vs concentration of methanol vapours.

nanocomposite can be attributed to the adsorption and desorption of the analyte vapours during the on-off cycle. The incorporated Pd nanoparticles play a significant role by catalyzing this phenomenon due to their surface activities. This results in a sharp increase in the resistance of the nanocomposite in methanol environment. As these interactions are purely physical in nature, desorption of the analyte molecules occurs within a few seconds. These results are further supported by the FT-IR studies.

Figure 4.3 depicts the FT-IR spectra of the unexposed nanocomposite (Fig. 4.3 A) and that exposed to two extreme concentrations of methanol, i.e. 1 ppm and 2000 ppm (Fig. 4.3 B and C). The spectra for the intermediate concentrations are not included since they are observed to be similar as that exposed to 2000 ppm methanol, in accordance with the response mentioned earlier.

The peaks at $\sim 3600\text{--}3000\text{ cm}^{-1}$ and $3000\text{--}2800\text{ cm}^{-1}$ correspond to the --N-H and --C-H stretching vibrations of Pani, respectively. The bands due to aromatic stretching vibrations of C-N appear at $\sim 1294\text{ cm}^{-1}$, while the absorption peaks at ~ 1594 and 1490 cm^{-1} represent the quinoid (Q) and benzenoid (B) structures of the emeraldine phase of Pani. However, comparison of the FT-IR spectra of the exposed samples with that of the unexposed nanocomposite reveals two significant differences. The

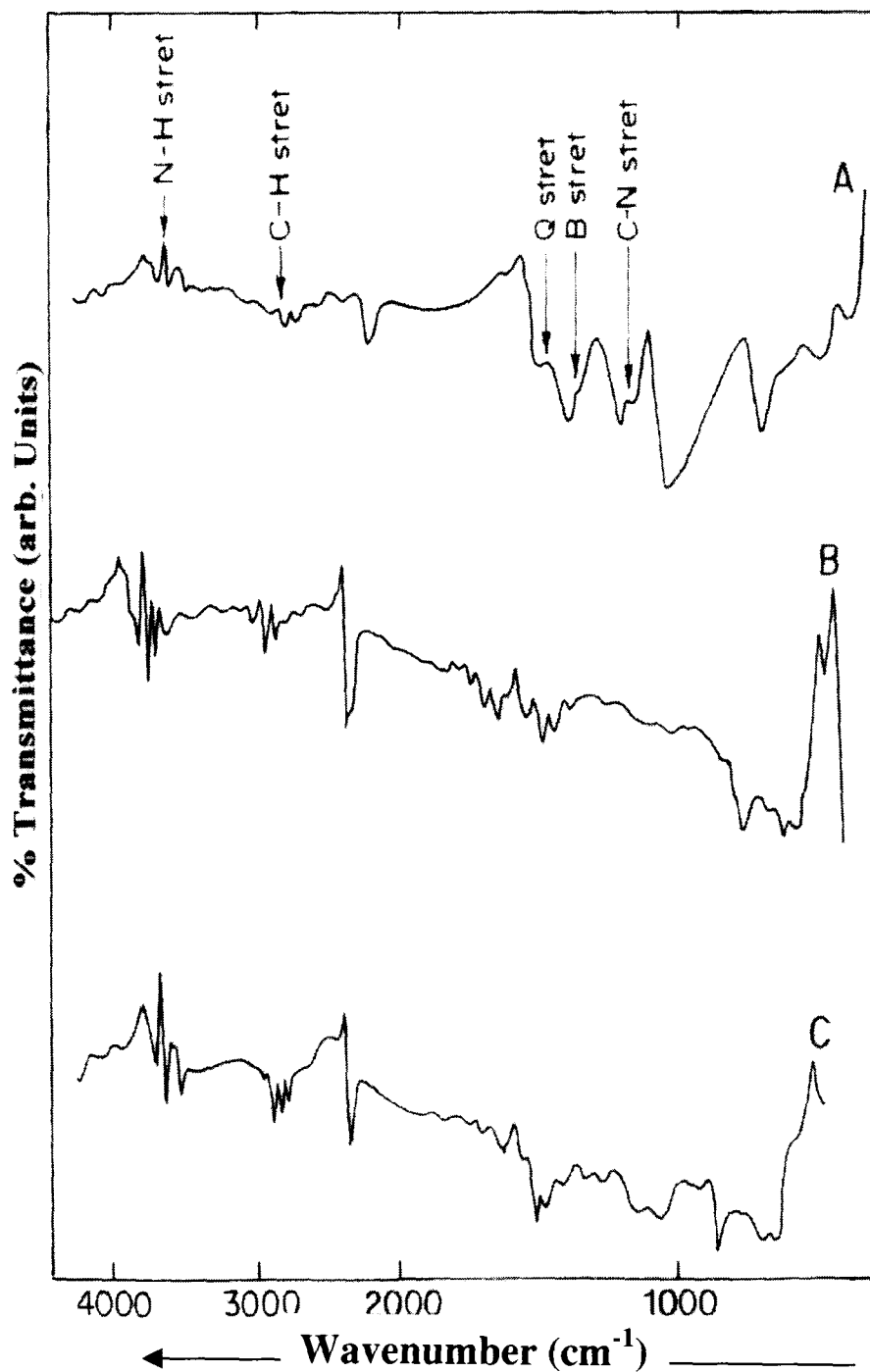
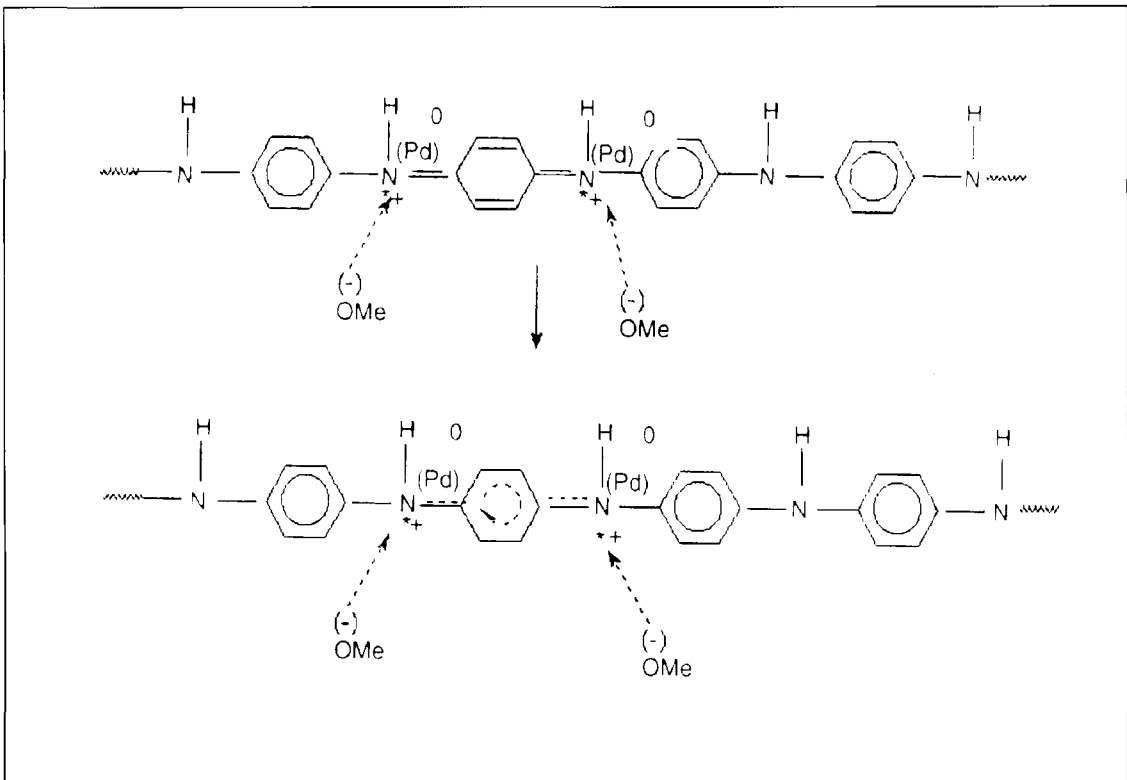


Fig. 4.3 FT-IR spectra of A) unexposed Pd-Pani nanocomposite and those exposed to various concentrations of methanol vapours such as B) 1 and C) 2000 ppm.

intensity as well as the sharpness of the peaks representing N-H and C-H stretching vibrations are found to be enhanced (the effect being more prominent at higher concentration of methanol, i.e. 2000 ppm). This could be due to the higher degree of interactions between these groups and the methanol molecules. Apart from this, the quinoid peak is seen to shift by $\sim 40 \text{ cm}^{-1}$ from 1594 cm^{-1} to 1550 and 1540 cm^{-1} on exposure to methanol vapours. This can be attributed to the interaction of the methanol molecules with the imine nitrogens, thereby causing the reducing effect. The effective positive charge on the imine nitrogen is reduced by the methanol molecules in the presence of Pd nanoparticles by converting the imine nitrogen to amine i. e. benzene-like structure is formed during the positive interaction. The reaction is shown in scheme 1. However, in the presence of air, methanol molecules are desorbed due to the moisture contained in air and the original peak frequencies can be observed in the FT-IR spectra.

The selectivity of the nanocomposite towards methanol vapours was investigated by exposing the sensor to mixtures of methanol + ethanol and methanol + isopropanol. The concentration of methanol in the mixtures was ~ 1500 ppm while that of ethanol and isopropanol were 700 and 900 ppm, respectively. The results show the magnitude of response to be identical as that observed for methanol. However, the response time is



Scheme 1. Schematic representation of sensing mechanism.

seen to increase appreciably from 2 to 12 min. The similarity in the magnitude of response at each concentration justifies that methanol molecules selectively adsorb on the nanocomposite, since methanol is more polar than ethanol and isopropanol and hence would interact more efficiently than the higher alcohols. The increase in response time can be attributed to the competition arising between the different molecules to be adsorbed over the nanocomposite. The bulkier molecules raise a barrier in diffusing towards the sensor, compared with the smaller methanol molecules.

Figure 4.4 shows the effect of aging on the response of the Pd-Pani nanocomposite after exposure to different concentrations of methanol measured up to 110 days. From the figure, the response ($\Delta R/R_0$) do not exhibit any significant change, maintaining its long term stability.

The Pd-Pani nanocomposite was found to be a highly sensitive and selective sensor for methanol vapours. The nanocomposite gave a stable response for a sufficiently long time.

4.3 Ag-Polyaniline Nanocomposite as an Ammonia Vapour Sensor :

The Ag-Pani nanocomposite pellet was subjected to various chemical vapours like alcohols, amines, chloroform and ammonia vapours to test its applicability as a sensor. The results revealed a selective response ($\Delta R/R_0$) of the nanocomposite towards ammonia vapours in terms of the

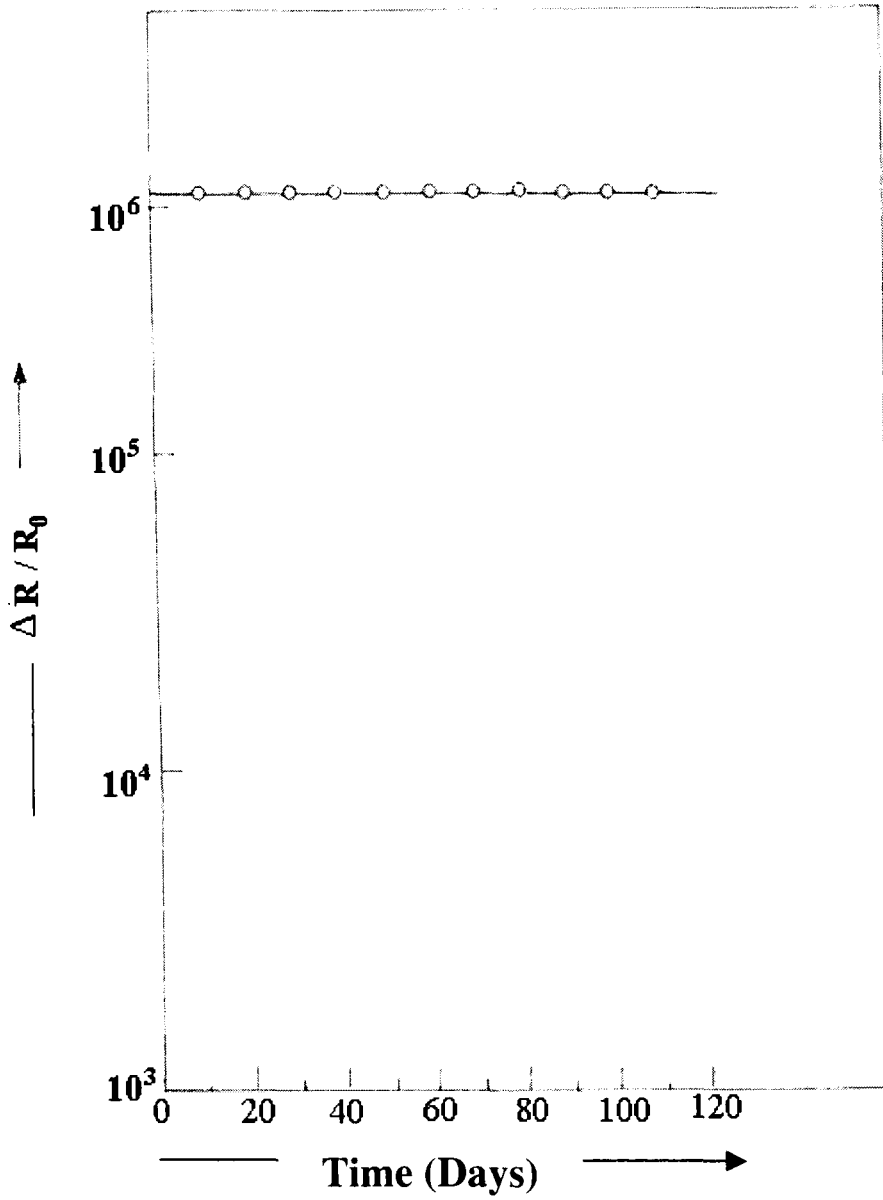


Fig. 4.4 A plot showing long term stability of Pd-Pani nanocomposite as methanol vapour sensor.

change in resistance of the order of 10^3 . The sensor exhibits reversible and reproducible response when measured up to 20 cycles. Further investigations were carried out by exposing the nanocomposite to different concentrations of ammonia from 1 to 600 ppm and the response was found to be linear up to 10 ppm ammonia concentration (Fig. 4.5 A-E) followed by saturation.

The response time is observed to be inversely proportional to the concentration of ammonia as seen in Fig. 4.6, curve 1. Sensitivity of the Ag-Pani nanocomposite as calculated from the plot of resistance vs concentration (Fig.4.6, curve 2) is $6.6 \times 10^2 \text{ k}\Omega\text{ppm}^{-1}$ which is in well agreement with the theoretical sensitivity value. Long term stability of the response up to a period of 60 days is found to be exhibited by the nanocomposite. The sensing mechanism involves adsorption–desorption phenomena during the on-off cycles. The FT-IR spectral data of exposed and unexposed Ag-Pani nanocomposite is given in Table 4.2.

The FT-IR spectral data of exposed samples when compared with that of the unexposed one, notable changes are observed in the quinoid and benzenoid band positions (Fig. 4.7). This could be due to the weak interactions between Ag^0 and the quinoid and benzenoid structures of the polymer matrix. The band corresponding to the benzenoid structure ($\sim 1486 \text{ cm}^{-1}$) is found to shift towards lower energy with increased

Table 4.2 FT-IR Spectral Data of Ag-Pani Nanocomposite Before and After Exposure to Ammonia Vapours.

Unexposed Ag-Pani	Ammonia concentration (ppm)				Peak Assignment
	1	10	100	600	
649	618	616	616	616	Out of plane -C-H bending vibrations.
809	800	806	807	809	Paradisubstituted benzene ring.
1145	1120	1119	1119	1118	B-N ⁺ H-B stretching vibrations.
1299	1291	1292	1293	1292	Aromatic (C-N) stretching band.
1486	1400	1401	1401	1401	Benzenoid ring stretching.
1571	1547	1560	1585	1587	Quinoid ring stretching band.
2920	2916	2918	2923	2915	-C-H stretching band.
3100-3700	3110	3116	3123	3127	-N-H stretching band.

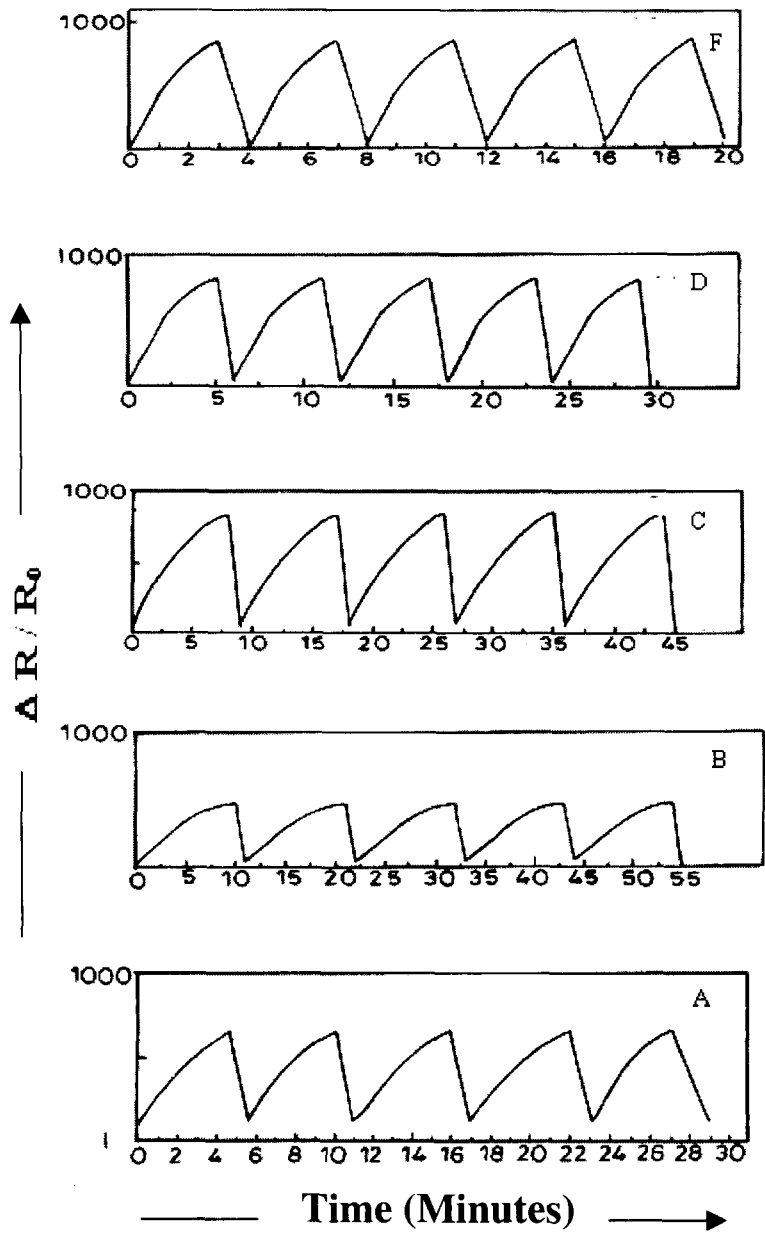


Fig. 4.5 Blank Pani exposed to A) 600 ppm and Ag-Pani nanocomposite exposed to B) 1, C) 10, D) 100 and E) 600 ppm concentrations of ammonia.

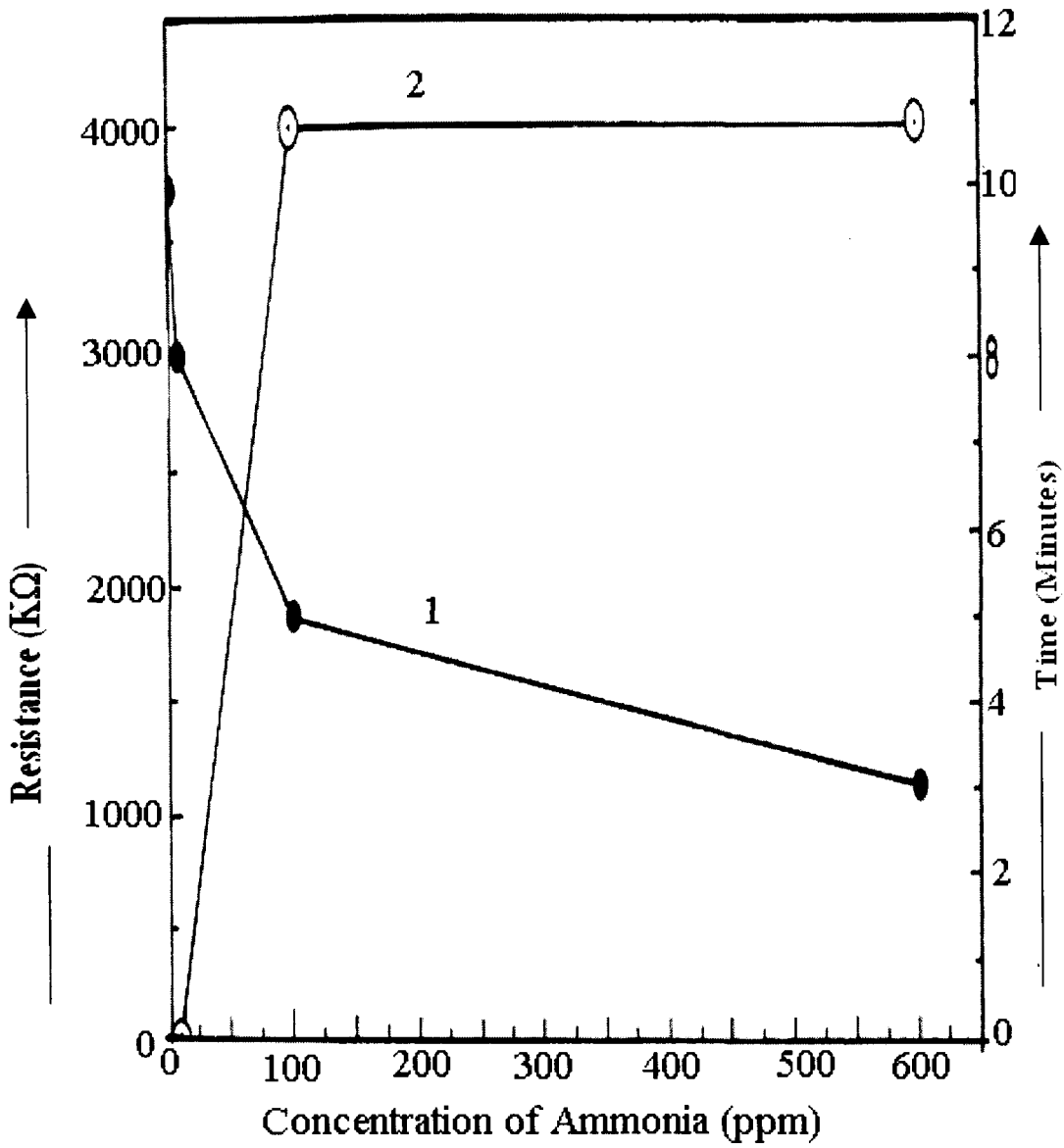


Fig. 4.6 A plot of concentration of ammonia vs 1) response time and 2) resistance.

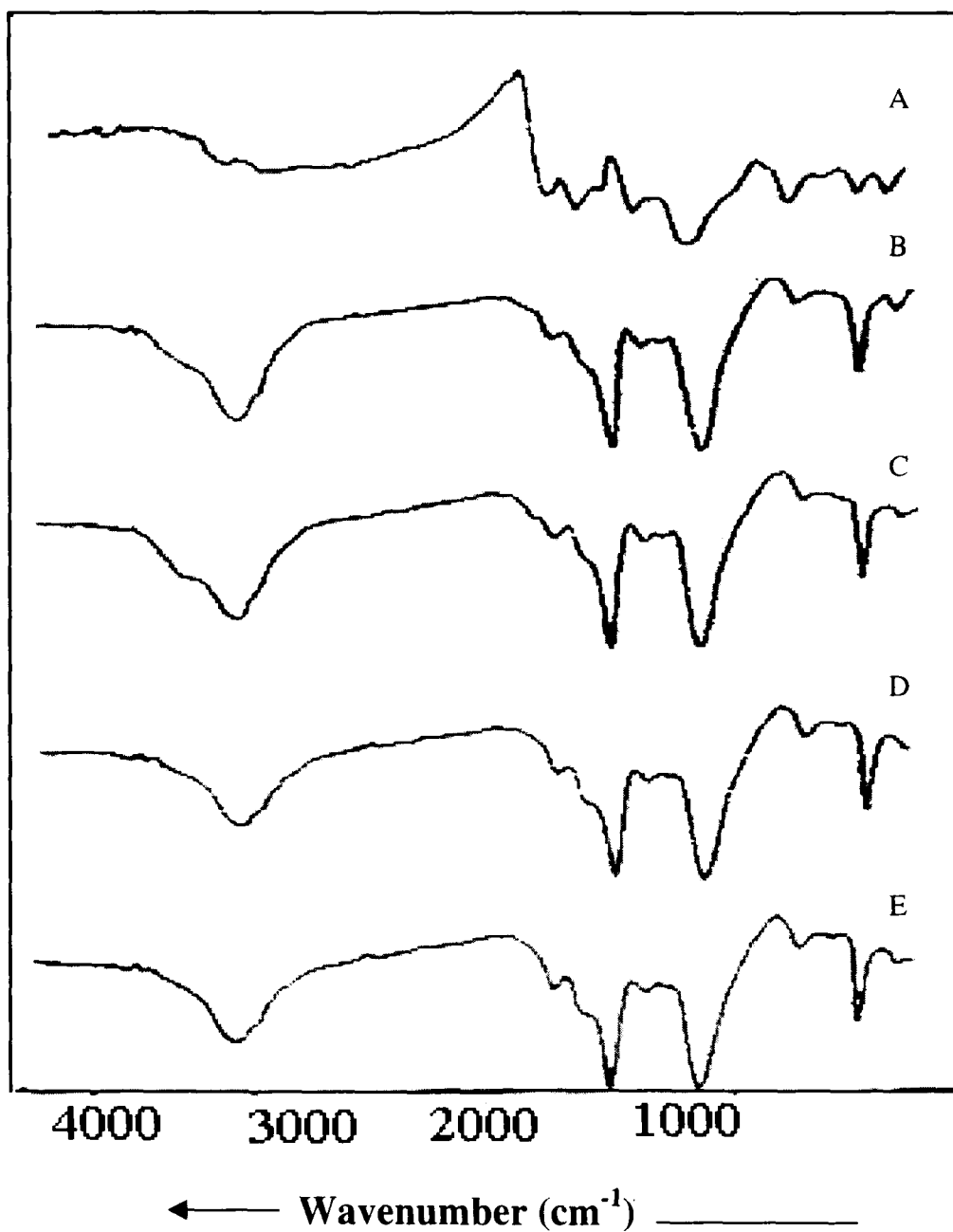


Fig. 4.7 Blank Pani exposed to A) 600 ppm and Ag-Pani nanocomposite exposed to B)1, C) 10, D) 100 and E) 600 ppm concentrations of ammonia.

intensity and sharpness in ammonia environment. Similarly, the nanocomposite when exposed to ammonia exhibit a shoulder at $\sim 1487\text{ cm}^{-1}$ corresponding to the ammonium ion. Increase in the intensities of B-N⁺H-B peak (1120 cm^{-1}) and the broad band at $3100\text{-}3700\text{ cm}^{-1}$ is observed with increase in the concentration of ammonia. The sensing behaviour can be associated with these changes in the peak positions which occur on adsorption, but revert to their original values during desorption of ammonia from the nanocomposite surface.

Ag-Pani composite is found to be a selective sensor for ammonia vapours.

4.4 Au-Polyaniline Nanocomposite as a Methanol Vapour Sensor :

Au-Pani nanocomposite pellets were used for sensing saturated vapours of different aliphatic alcohols such as methanol, ethanol and isopropanol. From the Fig. 4.8 it was observed that, the nanocomposite exhibited best response to methanol vapours. Therefore, further experiments related to the sensing measurements were carried out for various concentrations of methanol (1 to 800 ppm). The response was found to be highly reproducible and reversible when measured up to 20 cycles by switching between alcohol and air.

Figure 4.8 shows the nature of response exhibited by Au-Pani nanocomposite exposed to different concentrations of methanol along

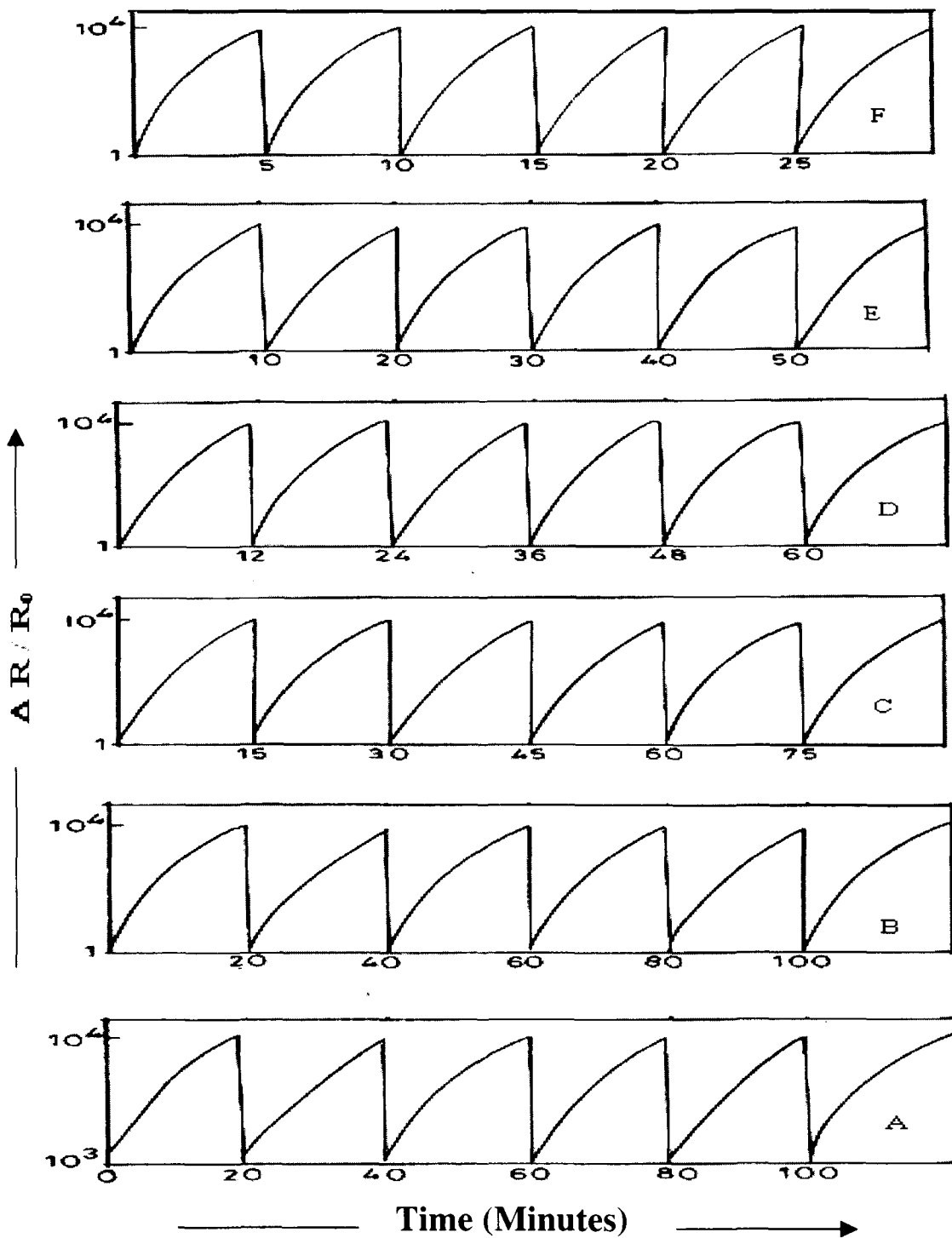


Fig. 4.8 Blank Pani exposed to A) 600 ppm and Au-Pani nanocomposite exposed to B) 1, C) 5, D) 10, E) 100 and F) 600 ppm concentrations of methanol.

with the blank Pani. The response ($\Delta R/R_0$) is relatively weak at 1 ppm methanol concentration. The magnitude of response is seen to increase with concentration up to 10 ppm. Beyond 10 ppm concentration the ($\Delta R/R_0$) is observed to be constant.

Further, the response time was found to decrease from 12 to 5 min. with increasing concentration of methanol (Fig.4.9 a).

The sensitivity of the nanocomposite calculated from the Fig. 4.9 b representing a plot of resistance vs. concentration of methanol is $1.29 \times 10^6 \Omega \text{ ppm}^{-1}$ which agrees well with the sensitivity determined theoretically i.e. $1.06 \times 10^6 \Omega \text{ ppm}^{-1}$. Above 10 ppm concentration of methanol the sensitivity appears to be constant.

Further, the selectivity of the nanocomposite is investigated by measuring the response of the nanocomposite by exposing it to mixtures of (methanol + ethanol) and (methanol + isopropanol vapours) (concentrations varying from 1 to 800 ppm). The response is observed to be identical (Figure not included) except that the time interval required increases from 5 to 20 min. as observed in Table 4.3.

Figure 4.10 depicts the FT-IR spectra of the Au-Pani nanocomposite exposed to various concentrations of methanol such as 1, 10, 50, 100 and 800 ppm together with the spectrum of unexposed Au-Pani

Table 4.3 Response Time of Methanol In Presence of Other Alcohols.

Concentration of Alcohol (ppm)	Response Time (Minutes)		
	Methanol	Ethanol	Isopropanol
1	20	32	45
10	15	25	36
50	12	20	29
100	10	15	20
800	5	10	15

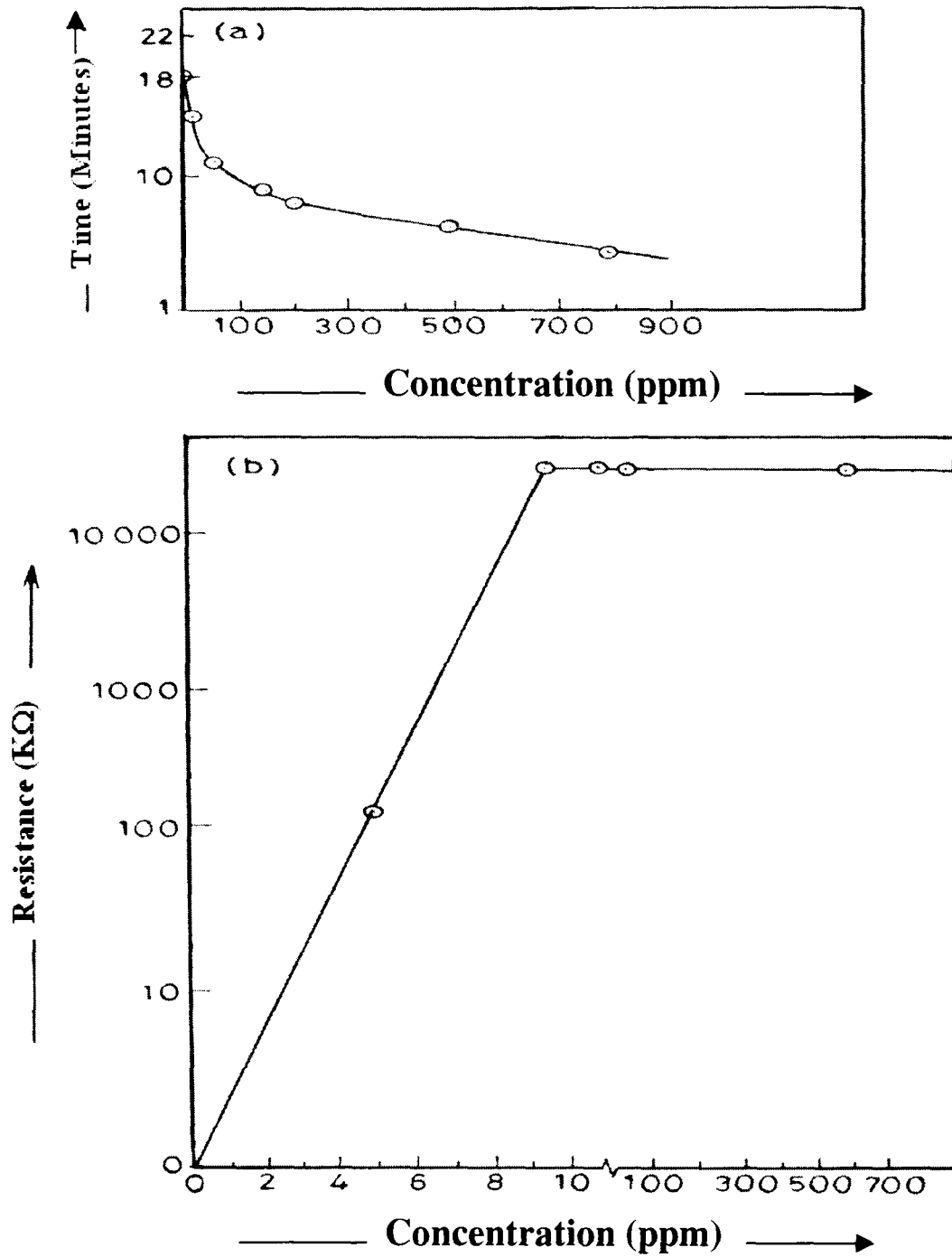


Fig. 4.9 A plot of concentration of methanol vapour against a) response time and b) resistance of Au-PANI nanocomposite.

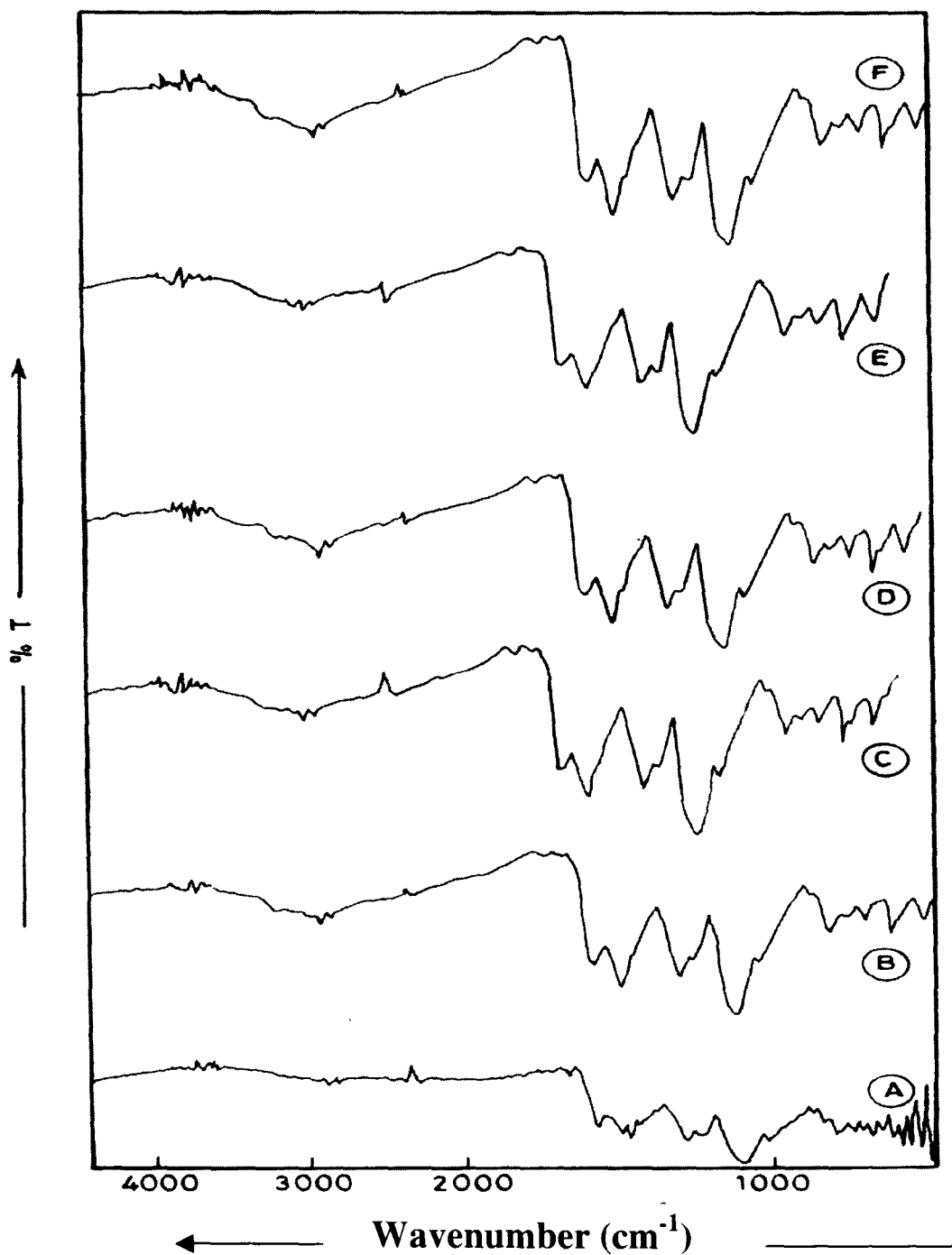


Fig. 4.10 FT-IR spectra of A) unexposed Au-Pani nanocomposite along with the nanocomposite exposed to concentration of B) 1, C) 5, D) 10, E) 100 and F) 600 ppm methanol.

nanocomposite. The major adsorption bands of the nanocomposite having usual significance are described in Table 4.4 [99-101].

The presence of peak at $\sim 3583\text{ cm}^{-1}$ in case of exposed nanocomposite spectra is indicative of -O-H vibration of methanol. Broadening of the peak was observed with the increasing concentration of methanol. This peak is absent in unexposed nanocomposite which is clearly seen from Figure 4.10, curve A. Broadening of the peak with increasing concentration of methanol suggests the increase in the extent of adsorption of methanol molecules over the nanocomposite surface. Comparison of spectra (Figure 4.10 B-F) with the unexposed spectrum shows significant modifications in various vibrational frequencies. A new peak at $\sim 2850\text{ cm}^{-1}$ corresponding to -C-H stretching vibrations becomes prominent confirming the adsorption of methanol vapours on nanocomposite. Further, the adsorption band at $\sim 2909\text{ cm}^{-1}$, 1478 cm^{-1} corresponding to benzenoid stretching (B) are observed to be shifted towards higher frequencies whereas, quinoid stretching (Q) vibration frequency ($\sim 1585\text{ cm}^{-1}$) shows a reverse behaviour.

Au-Pani nanocomposite is found to be highly sensitive to methanol vapours. The selectivity is seen to be rendered to the nanocomposite by the Au metal nanoparticles. Au-Pani nanocomposite is observed to be suitable for detecting low ppm concentrations (upto 10 ppm) of methanol.

Table 4.4 FT-IR Spectral Data of Au-Pani Nanocomposite Before and After Exposure to Various Concentrations of Methanol.

Unexposed Au-Pani nanocomposite	Methanol concentration (ppm)					Peak Assignment
	1	10	50	100	800	
3100-3700	3100-3700	3100-3700	3100-3700	3100-3700	3100-3700	-N-H stretching band
-	3583.0	3583.3	3580.9	3582.3	3580.4	-O-H stretching
2909.0	2916.8	2915.3	2918.7	2912.8	2918.1	-C-H stretching band
1585.4	1574.6	1574.5	1571.2	1576.4	1571.3	Quinoid ring stretching
1510.2	-	-	-	-	-	N-B-N stretching
1478.4	1490.6	1486.4	1488.1	1487.3	1488.7	Benzenoid stretching
1296.2	1298.0	1297.6	1298.0	1297.7	1298.0	Aromatic (C-N) stretching band
1108.7	1114.2	1113.0	1112.2	1114.2	1112.3	B-N ⁺ -H-B stretching vibration
813.9	815.8	816.1	819.4	810.7	817.6	Paradisubstituted
756.8	757.1	756.9	-	-	-	Out of plane -C-H bending vibration
639.9	693.8	693.9	692.5	694.0	693.3	-C-H out of plane on 1,2 ring
628.0-505.6	615.1-507.2	615.6-505.5	616.1-506.4	614.1-506.4	616.1-506.4	Aromatic deformation